frontiers in Materials

ORIGINAL RESEARCH
published: 21 February 2022
doi: 10.3389/fmats.2022.849601

Microstructure and Mechanical Properties of $Li_2Si_2O_5$ Whisker-Reinforced Glass-Ceramics

Jingyu Yan[1,2†], *Xiaoming Liu*[1,2†], *Xiuping Wu*[1,2], *Xiao Wu*[1,2], *Yanjie Zhang*[3] *and Bing Li*[1,2*]

[1]*Shanxi Medical University School and Hospital of Stomatology, Taiyuan, China,* [2]*Shanxi Province Key Laboratory of Oral Diseases Prevention and New Materials, Taiyuan, China,* [3]*Research Institute of Photonics, Dalian Polytechnic University, Dalian, China*

Lithium disilicate ($Li_2Si_2O_5$) glass-ceramics are an ideal material for dental restoration; however, their intrinsic brittleness and low defect tolerance limit the scope of their clinical applications. In this study, $Li_2Si_2O_5$ whiskers were creatively synthesized via a mild-condition hydrothermal reaction. Self-reinforced $Li_2Si_2O_5$ glass-ceramics were sintered by introducing the $Li_2Si_2O_5$ whiskers, and their effects on phase, microstructure, and mechanical properties were systematically studied. The crystal-growth and toughening mechanisms were also discussed. The results showed that the $Li_2Si_2O_5$ whiskers played an important role in inducing crystallization, and improving the microstructure and properties of the glass-ceramics. With increasing amounts of $Li_2Si_2O_5$ whiskers, the crystallinities increased slightly, and the average crystal size also increased. The microstructure was composed of crystals of bimodal size distributions, in which some large, rod-like $Li_2Si_2O_5$ crystals epitaxially grew along with the whiskers, and small crystals directly crystallized from the parent glass-ceramic powders. The $Li_2Si_2O_5$ glass-ceramics exhibited high flexural strength (389.5 ± 11.77 MPa, LDW3), and fracture toughness (3.46 ± 0.10 MPa·$m^{1/2}$, LDW5). The improved properties were attributed mainly to crack deflection and bridge-toughening mechanisms.

Keywords: lithium disilicate, glass-ceramics, dental restoration, whiskers, microstructure, mechanical properties

Edited by:
Laijun Liu,
Guilin University of Technology, China

Reviewed by:
Shiv Prakash Singh,
International Advanced Research Centre for Powder Metallurgy and New Materials, India
Pengrong Ren,
Xi'an University of Technology, China
Li Zeng,
Chengdu University, China

****Correspondence:***
Bing Li
libing1975vip@163.com

†These authors have contributed equally to this work and share first authorship

Specialty section:
This article was submitted to Ceramics and Glass, a section of the journal Frontiers in Materials

Received: *06 January 2022*
Accepted: *07 February 2022*
Published: *21 February 2022*

Citation:
Yan J, Liu X, Wu X, Wu X, Zhang Y and Li B (2022) Microstructure and Mechanical Properties of $Li_2Si_2O_5$ Whisker-Reinforced Glass-Ceramics. Front. Mater. 9:849601. doi: 10.3389/fmats.2022.849601

1 INTRODUCTION

$Li_2Si_2O_5$ glass-ceramics are a kind of dental restoration material with $Li_2Si_2O_5$ as the main crystalline phase, which has suitable mechanical properties and aesthetical characteristics owing to its unique crystal properties and distribution (Montazerian and Zanotto, 2017; Fu et al., 2020). These glass-ceramics are considered promising candidates for restorative dentistry applications. However, owing to their intrinsic brittleness and low defect tolerance, it has been claimed that these materials also exhibit several disadvantages (Huang et al., 2014; Kwon et al., 2018; Zhang et al., 2019). As a result, it is necessary to improve the fracture toughness of $Li_2Si_2O_5$ glass-ceramics, which have very important practical significance for large-scale applications in the field of prosthodontics.

Many researchers have attempted to improve the fracture toughness of $Li_2Si_2O_5$ glass-ceramics by changing their heat-treatment process and using different nucleating agents (Huang et al., 2014; Lien et al., 2015; Wang et al., 2015; Sun et al., 2021), but with unsatisfactory results. $Li_2Si_2O_5$ glass-ceramics have been prepared by melting and powder sintering methods. The difference between the two routes lies in their crystallization mechanism: the melting method involves overall crystallization to obtain high-density materials, while the sintering method is beneficial to the surface crystallization

of glass powders and can produce glass-ceramic materials with a high crystallization degree (Albakry et al., 2004; Hallmann et al., 2019; Zhao et al., 2019). However, no matter which method is used to prepare $Li_2Si_2O_5$ glass-ceramics, the crystalline phase precipitates from the parent glass, and the formation and growth of the crystal nucleus are controlled by the nucleating agent used and the high specific surface area of the glass powders. Therefore, $Li_2Si_2O_5$ crystals prepared by these two traditional methods usually have small particle sizes (Hallmann et al., 2018). The presence of these small crystals leads to a high interfacial area and a lack of interlocking structures between crystals, resulting in more microcracks and poor crack-propagation resistance (Li et al., 2016; Belli et al., 2018; Zhang Z. et al., 2018).

Several methods have been successfully employed to strengthen and toughen glass-ceramics such as the addition of zirconia into the glass composition (Huang et al., 2014). The improved properties are mainly attributed to compressive stress reinforcement, phase transformation, and bridging toughening mechanisms (Huang et al., 2014; Elsaka and Elnaghy, 2016; Hussain et al., 2021). However, the introduction of zirconia presents some disadvantages, such as uneven dispersion of the second phase, difficulty in densification, and poor machining performance (Zhang et al., 2019; Chen et al., 2020).

Whiskers are a kind of tiny single crystal with a large aspect ratio and fewer structural defects, such as silicon nitride, magnesium oxide, carbon nanofibers. Their diameter is generally at the nanometer level, and their length can reach the micron level (Liang et al., 2017; Zhang Y. et al., 2018). The addition of whiskers to ceramic material can improve the material properties of the latter through crack deflection, crack bridging, and pull-out effects (Zhang Y. et al., 2018). For $Li_2Si_2O_5$ glass-ceramics, cracks usually occur at the weak interface between crystals and through the residual glass matrix (Zheng et al., 2008; Yuan et al., 2013; Kirsten et al., 2020; Leenakul and Kraipok, 2021). Nevertheless, few studies on $Li_2Si_2O_5$ whisker-reinforced glass-ceramics have been performed. Therefore, our aim is to improve the properties of $Li_2Si_2O_5$ glass-ceramics by adding large $Li_2Si_2O_5$ whiskers.

In this paper, $Li_2Si_2O_5$ whiskers were synthesized via a mild-condition hydrothermal reaction, and different amounts of the whiskers were added to the glass composition to prepare high-performance $Li_2Si_2O_5$ glass-ceramics with elongated, rod-like $Li_2Si_2O_5$ crystals. The effects of adding the $Li_2Si_2O_5$ whiskers on the glass-ceramic phase, microstructure, and mechanical properties were systematically studied, and the crystal-growth and toughening mechanisms were also discussed.

2 MATERIALS AND METHODS

2.1 Preparation of the $Li_2Si_2O_5$ Whiskers

The $Li_2Si_2O_5$ whiskers were synthesized in a one-step hydrothermal process. The molar mass proportion of $LiOH{\cdot}H_2O$ to $SiO_2{\cdot}H_2O$ was maintained at 1:1 according to the stoichiometric composition. After mixing the constituents, batches were dissolved in deionized water for 4 h. The resultant solutions were transferred and sealed in a Teflon-lined stainless-steel autoclave under autogenous pressure and heated to 150°C for 6 h. The solutions were then cooled naturally to room temperature, sieved, washed several times in turn with distilled water and ethanol, and finally dried at 80°C for 24 h; the resultant white precipitates were recovered. The detailed process is the same as our previous studies (Liu et al., 2022).

TABLE 1 | Composition of the base glass (Unit: mol%).

SiO_2	Li_2O	P_2O_5	K_2O	Al_2O_3	La_2O_3
65.5	27.5	1.2	1.8	2	2

2.2 Preparation of the $Li_2Si_2O_5$ Glass-Ceramics

Reagent-grade powders of Li_2CO_3, SiO_2, $NH_4H_2PO_4$, Al_2O_3, K_2CO_3, and La_2O_3 were used as raw materials. The composition of the base glass is given in **Table 1**. After mixing the constituents, batches were placed in a Pt crucible and melted in an electric furnace at 1,450°C for 30 min in air. Then, the glass melts were quenched in deionized water to obtain frits for milling. The dried glass frits were ball milled with high-purity zirconia balls in an ethanol environment. The blended powders were washed and then dried to obtain glass powders (Liu et al., 2022).

To investigate their crystallization effect on glass-ceramics, $Li_2Si_2O_5$ whiskers (0, 1, 3, and 5 wt%) were then added to the glass powders. These glasses were represented as LDW0, LDW1, LDW3, and LDW5, respectively. The glasses were wet-mixed with zirconia balls in 99.7% anhydrous alcohol for 2 h. After drying, the mixtures were placed in a hardened-steel die and uniaxially pressed under 20 MPa. Then, the samples were sintered in a vacuum furnace at 900°C for 1.5 h. Finally, after cooling to ambient temperature, the surface layers of the samples were removed for subsequent characterization.

2.3 Characterization

The crystalline phases of the samples were characterized by X-ray diffraction analysis (XRD-7000S, Japan) using Cu-Kα radiation with a scanning velocity of 5°/min, a step width of 0.02°, a scanning range of 10–60°, an acceleration voltage of 40 kV, and a current of 30 mA. In addition, the relative crystallinities of the samples were calculated by Jade 6.0 software using the number, relative intensity, and location of diffraction peaks according to the XRD pattern. The relative crystallinity of the glass-ceramics is estimated according to the following equation:

$$X_c = \frac{\sum I_c}{\sum I_c + KI_a} \times 100\% \quad (1)$$

where *Xc* is the crystallinity, *Ic* is the integrated intensity of the crystal diffraction peaks, *Ia* is the integrated intensity of the amorphous fraction, and K is a constant related to the measurement conditions and glass compositions.

The $Li_2Si_2O_5$ glass-ceramic samples were polished and etched using a 10 vol% HF solution for 15 s, and their microstructures were observed by scanning electron microscopy (SEM,

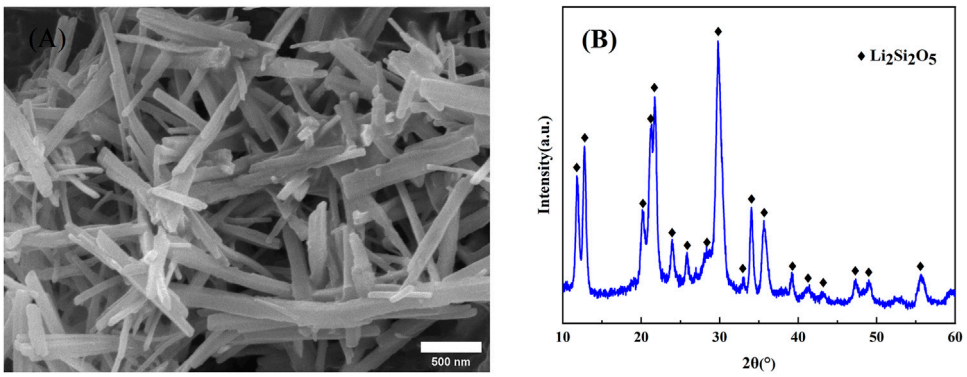

FIGURE 1 | (A) SEM image and **(B)** XRD pattern of the $Li_2Si_2O_5$ whiskers. Adapted with permission from (Liu et al., 2022).

JSM6701F, Japan). The three-point flexural strength of the specimens (24 mm × 4 mm × 1.5 mm after chamfering, smoothing, and polishing) was determined by a universal mechanical machine (Instron 3366, United States) with a span (center-to-center distance between support rollers) of 16 mm and a crosshead speed of 0.5 mm/min according to ISO 6872. Ten test bars were prepared to obtain average values. The three-point flexure is calculated using the following equation:

$$\sigma = \frac{3Pl}{2wb^2} \tag{2}$$

where σ is the flexural strength in units of MPa, P is the breaking load in N, and l, w, and b represent the sample test span, width, and thickness in mm respectively.

The fracture toughness of the specimens (24 mm × 4 mm × 3 mm) was measured following the single-edge V-notched beam (SEVNB) method. A U-shaped groove was notched at the surface of the 3 × 24 mm side with a diamond cutting wheel cooled with water, and a V-shaped notch with a tip radius of less than 15 μm was machined on the bottom of the groove. The notched side of the bar was placed under tension in the three-point bending apparatus with a span of 16 mm and a crosshead speed of 0.5 mm/min. Fracture toughness tests were carried out for each group of five samples per group of glass-ceramic specimens to verify accuracy and dispersion.

3 RESULTS AND DISCUSSION

3.1 Characterization of the $Li_2Si_2O_5$ Whiskers

The SEM morphology and XRD pattern of the $Li_2Si_2O_5$ whiskers synthesized by the hydrothermal method are shown in **Figures 1A,B**, respectively. It was clearly observed that the $Li_2Si_2O_5$ whiskers were rod-like crystals with an average length of 1.37 ± 0.23 μm, width of 0.13 ± 0.02 μm, and aspect ratio of 5–12 (**Figure 1A**). XRD analysis showed no impurity peaks, as seen in **Figure 1B**, indicating that the obtained samples had high purity, and the diffraction peaks were consistent with those of

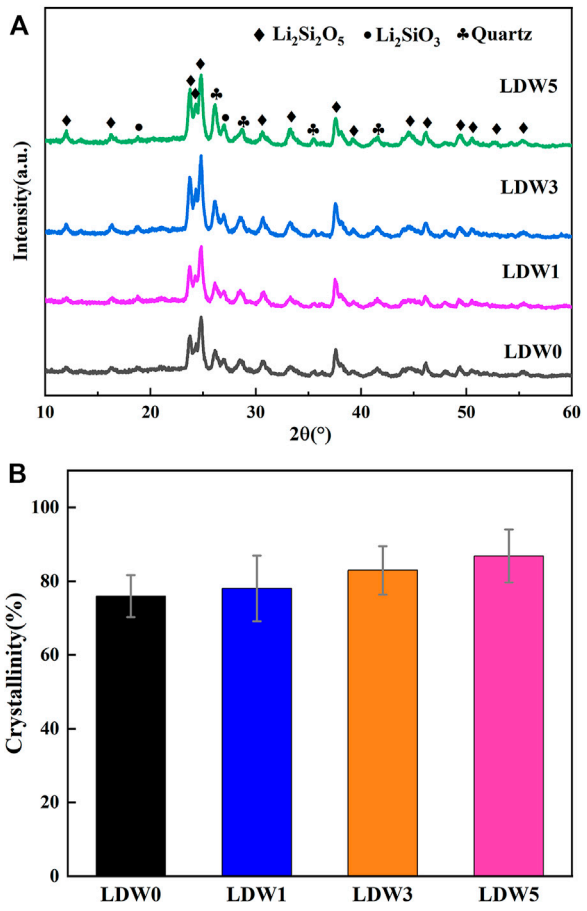

FIGURE 2 | (A) XRD patterns and **(B)** crystallinity of the $Li_2Si_2O_5$ glass-ceramics with different compositions.

ICDD PDF #33-0816 (Liu et al., 2022). Therefore, the synthesis of the $Li_2Si_2O_5$ whiskers by the hydrothermal method laid the foundation for the subsequent $Li_2Si_2O_5$ whisker-reinforced glass-ceramic. In this work, we report a simple hydrothermal approach for the synthesis of $Li_2Si_2O_5$ whiskers with regular, new

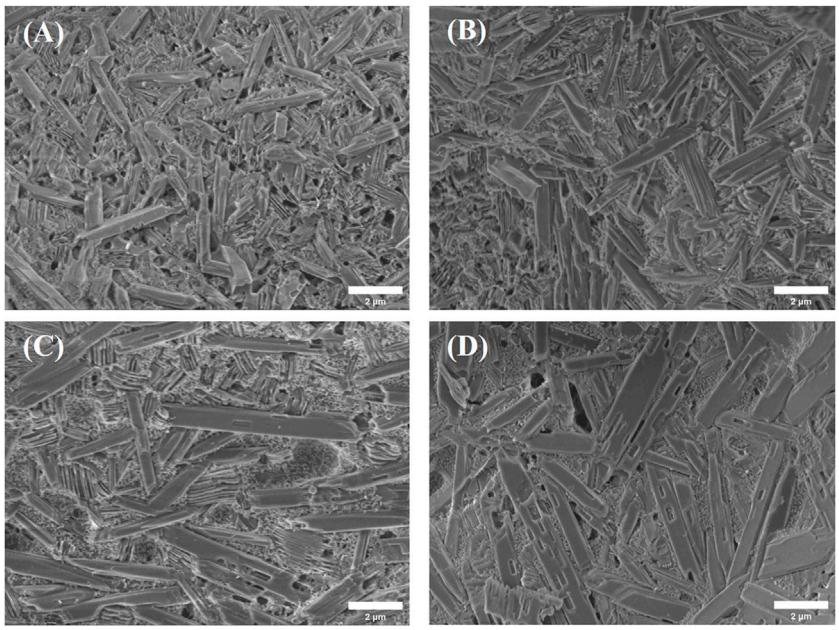

FIGURE 3 | SEM images of the $Li_2Si_2O_5$ glass-ceramics with different compositions: **(A)** LDW0; **(B)** LDW1; **(C)** LDW3; and **(D)** LDW5.

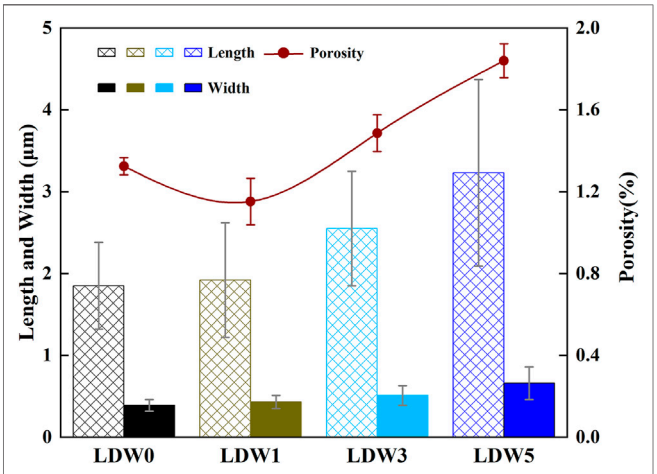

FIGURE 4 | Grain size and porosity of the $Li_2Si_2O_5$ glass-ceramics with different compositions.

morphology. At present, the hydrothermal method has broad application prospects in the synthesis of nanophase materials under low-temperature conditions. The hydrothermal method is environmentally friendly, as its reaction is carried out under closed-system conditions, saving energy (Alemi et al., 2014a; Alemi et al., 2014b).

3.2 Phase Formation

XRD patterns of the $Li_2Si_2O_5$ glass-ceramics are shown in **Figure 2A**. The main precipitated crystalline phase of all samples was $Li_2Si_2O_5$ (ICDD PDF#40-0376). With an increase in the amount of $Li_2Si_2O_5$ whiskers, the intensity of the diffraction peaks of the $Li_2Si_2O_5$ crystals shifted slightly, owing to changes in crystallinity and crystal size. Under an identical preparation process, the intensity of the diffraction peaks of the $Li_2Si_2O_5$ crystals increased slightly from LDW0 to LDW5. As seen in **Figure 2B**, the crystallinity of the samples remained relatively constant (from 75.98 ± 5.72% to 78.09 ± 8.89%) upon varying the whisker content from 0 to 1 wt%, while it increased significantly to 86.86 ± 7.18% in LDW5.

Enormous efforts have been made to optimize the $Li_2Si_2O_5$ crystals embedded in glass-ceramics in multicomponent systems with nucleating agents or glass modifiers. Among these additives, P_2O_5 is known to be the most effective for increasing the nucleation rate since it promotes the bulk nucleation of $Li_2Si_2O_5$ by forming a steep compositional gradient in the vicinity of the amorphous Li_3PO_4 phase, where it acts as the heterogeneous nucleation site for both Li_2SiO_3 and $Li_2Si_2O_5$ phases (Clausbruch et al., 2000; Huang et al., 2013). As for the Al_2O_3 component, it can reduce phase-separation trends and increase thermal stability, and a small amount is beneficial for improving the crystallization controllability of the Li_2O–SiO_2 system (Thieme and Rüssel, 2014). As for K_2O, it can promote the rupturing of bridging oxygen bonds between silicon and oxygen tetrahedrons, improving the O/Si ratio in the system, which is conducive to the precipitation of Li_2SiO_3 crystals (Fernandes et al., 2012). In addition, La_2O_3 can be added to reduce the viscosity of the glass system.

In this study, phase separation was promoted during the crystallization heat treatment to form Li-rich and Si-rich phases, after the addition of P_2O_5 to the $Li_2Si_2O_5$ glass system. Li_2O interacts with P_2O_5 in the Li-rich regions to form Li_3PO_4 crystal nuclei, which can occur at non-uniform nucleation sites of

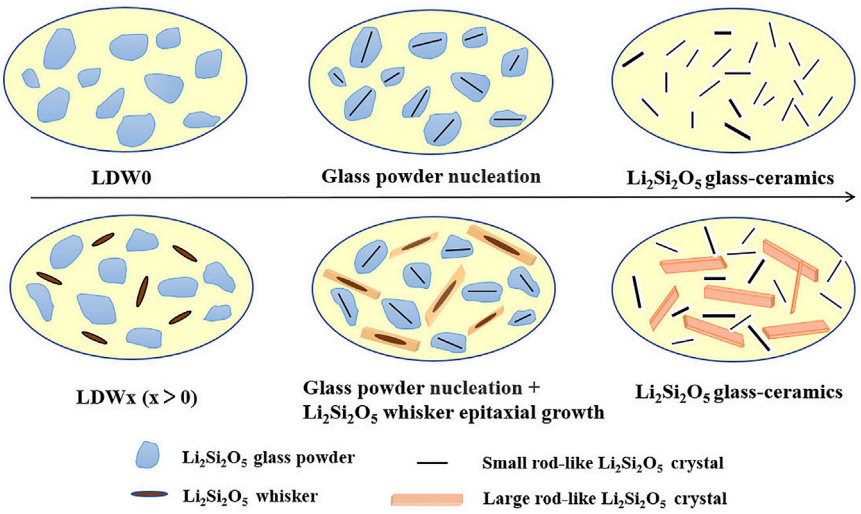

FIGURE 5 | Crystallization models of the $Li_2Si_2O_5$ glass-ceramics with and without $Li_2Si_2O_5$ whiskers.

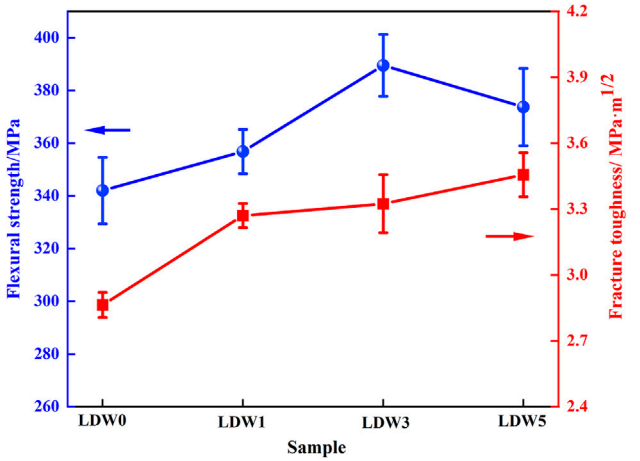

FIGURE 6 | Flexural strength and fracture toughness of the $Li_2Si_2O_5$ glass-ceramics with different compositions.

Li_2SiO_3 and $Li_2Si_2O_5$ crystals according to the following reaction scheme, which was conducive to reducing the nucleation energy (Wen et al., 2007; Lodesani et al., 2020).

$$P_2O_5\,(glass)+3Li_2O\,(glass)=\ 2Li_3PO_4\,(crystal) \quad (3)$$

$$Li_2O\,(glass)+SiO_2\,(glass)=\ Li_2SiO_3\,(crystal) \quad (4)$$

$$Li_2SiO_3\,(crystal)+SiO_2\,(glass)=\ Li_2Si_2O_5\,(crystal) \quad (5)$$

Upon increasing the amount of $Li_2Si_2O_5$ whiskers, the whisker content in the Li-rich regions also increased. The added $Li_2Si_2O_5$ whiskers could act as nuclei sites, so the simultaneous effect of surface nucleation from the glass powders and that induced by the whiskers increased the degree of crystallization (Zhao et al., 2021). Consequently, the nucleation rate rose, and the crystallinity increased.

Although pure SiO_2 glass crystallizes above 1,000°C, a small amount of quartz appeared at lower temperatures in this study. This was because Li_3PO_4 and the added $Li_2Si_2O_5$ whiskers may have provided some heterogeneous nucleation sites to induce the crystallization of quartz (Zhao et al., 2019).

3.3 Microstructure

The SEM morphologies of the $Li_2Si_2O_5$ glass-ceramics are shown in **Figure 3**. The $Li_2Si_2O_5$ crystals exhibited a closely packed and rod-like morphology, forming multi-directionally interlocking microstructures. However, the sizes of the crystals were quite different. The crystal sizes of the LDW0 samples were uniform, and no large crystals were found. In the LDW1, LDW3, and LDW5 samples, a bimodal crystal size distribution in which both large, elongated $Li_2Si_2O_5$ crystals and fine crystals existed was observed. This was because the surface nucleation of some whiskers began to occur, where the glass phase nucleates to form $Li_2Si_2O_5$ crystals on the surfaces of these whiskers. These crystals then grow from the interfaces between whiskers and the glass phase in the center of the adjacent glass region. The large rod-like $Li_2Si_2O_5$ crystals were believed to result from the epitaxial growth of the $Li_2Si_2O_5$ whiskers, while the small crystals were directly crystallized from the $Li_2Si_2O_5$ glass powders. The specific crystal size and porosity data are summarized in **Figure 4**. These results showed that the average length and width of the $Li_2Si_2O_5$ crystals increased from 1.85 ± 0.53 to 3.23 ± 1.14 μm and 0.39 ± 0.07 to 0.66 ± 0.2 μm, respectively, moving from LDW0 to LDW5. Further, the porosity increased after first decreasing. The lowest porosity of 1.15 ± 0.11% was obtained in the LDW1 sample.

The essence of the crystallization mechanism could be understood through the different samples with and without the $Li_2Si_2O_5$ whiskers, as compared in **Figure 5**. In the LDW0 specimen, the parent glass powders, with high surface energy,

TABLE 2 | Comparison of the mechanical properties of $Li_2Si_2O_5$ glass-ceramics between reported studies and the current study.

Author	Chemical composition	Thermal treatments	Flexural strength (MPa)	Fracture toughness K_{IC}/ ($MPa{\cdot}m^{1/2}$)
Wen et al. (2007)	31Li_2O, 62SiO_2, 2ZnO, 3K_2O, 1CaO, 1 P_2O_5 (mol%) Base-glass:	Hot-pressed at 820°C/1 h	290 ± 10 (TPBS)	3.3 ± 0.1 (SENB)
Huang et al. (2014)	62SiO_2, 31Li_2O, 2ZnO, 3K_2O, 1CaO, 1P_2O_5 (mol%) 85Base-glass + 15ZrO_2 (wt%) Base-glass:	Hot-pressed at 800°C/1 h	340 ± 38 (TPBS)	3.5 ± 0.3 (SENB)
Zhang et al. (2018a)	28.6Li_2O, 68.6SiO_2, 2K_2O, 0.8La_2O_3 (mol%) 90Base-glass + 10 mullite whiskers (wt%) Base-glass:	Sintered at 600°C/30 min + hot-pressed at 860°C/1 h	300 (TPBS)	2.7 (IF)
Zhao et al. (2019)	68.6SiO_2, 28.6Li_2O, 2.0K_2O, 0.8 La_2O_3 (mol%) Li_2SiO_3 crystals powder: SiO_2: Base-glass = 1:1.5:0.5 (in molar ratio) Base-glass:	Hot-pressed at 840°C/1 h	373 ± 12 (TPBS)	3.35 ± 0.12 (SEVNB)
Zhao et al. (2021)	68.6SiO_2, 28.6 Li_2O, 2K_2O, 0.8La_2O_3 (mol%) 95Baseglass + 5$Li_2Si_2O_5$ seeds (wt%) Base-glass:	Sintered at 800°C/20 min + hot-pressed at 850°C/0.5 h	396 ± 7 (TPBS)	3.31 ± 0.19 (SEVNB)
Our work	65.5SiO_2, 27.5Li_2O, 2Al_2O_3, 1.8K_2O, 2La_2O_3, 1.2P_2O_5 (mol%) 97Base-glass + 3$Li_2Si_2O_5$ whiskers (wt%) (LDW3) 95Base-glass + 5$Li_2Si_2O_5$whiskers (wt%) (LDW5)	Sintered at 900°C/1.5 h	389.5 ± 11.77 (TPBS)	3.46 ± 0.10 (SEVNB)

TPBS, three-point bending strength; SENB, single edge notch beam; IF, indentation fracture test; SEVNB, single-edge V-notched beam.

directly precipitated small, rod-like crystals. In the case of LDWx ($x > 0$), in addition to the glass powders, $Li_2Si_2O_5$ whiskers were added to induce crystallization and encourage epitaxial growth to form large, rod-like crystals, thus forming the coexistence of multi-scale crystals.

3.4 Mechanical Properties

The improvement in the mechanical properties of the samples was also a consequence of obtaining an appropriate microstructure, crystalline phase composition, and lower porosity. The flexural strength and fracture toughness of the four specimen groups are listed in **Figure 6**. Compared with the whisker-free glass-ceramics (LDW0), flexural strength was found to increase upon adding $Li_2Si_2O_5$ whiskers. With increasing whisker amount, the flexural strength increased and then decreased after its peak value, increasing from 356.8 ± 8.4 MPa for LDW1 to 389.5 ± 11.77 MPa for LDW3, then slightly decreasing for LDW5. The fracture toughness of the glass-ceramics strongly improved with the addition of the $Li_2Si_2O_5$ whiskers, reaching a maximum (3.46 ± 0.1 $MPa{\cdot}m^{1/2}$) for the LDW5 specimens.

Concerning the LDW0 sample, the flexural strength and fracture toughness were lower than those of LDW1, LDW3, and LDW5. Although the LDW0 sample had a relatively low porosity, its crystallinity was not high, and the sizes of its crystal distribution were concentrated, which cannot effectively hinder crack propagation and transfer interfacial stress. The flexural strength of the LDW3 sample was the highest. In part, this was because the crystallinity was more suitable, and the porosity was within an acceptable range. Further, the microstructure was more compact, and the average aspect ratio of the sample was suitable.

Micro residual stress existed in the $Li_2Si_2O_5$ glass-ceramics owing to the thermal expansion coefficient mismatch between the glass matrix and crystal (Pinto et al., 2007). At room temperature, there existed radial residual compressive stress in the crystal and tangential residual tensile stress in the glass matrix (Serbena and Zanotto, 2012; Serbena et al., 2015). With the increase of crystal size, the residual stress level increased (Li et al., 2016). In the three-point bending process, the residual tensile stress in the glass matrix overlapped with the macroscopic external tensile stress on the tension side of the specimen, which was beneficial to crack propagation in the glass matrix and reducing the bending fracture load. In this study, although LDW5 showed the highest crystallinity (86.86%), its flexural strength was not optimal. There were several reasons to explain these phenomena. Firstly, the coarse crystals were also controlled by the micro residual stress effect, the existence of which led to the decrease in strength. Secondly, increasing the amount of whiskers led to an increased porosity. Thus, the optimal flexural strength appeared in LDW3.

As for fracture toughness, the values of the glass-ceramics increased with the addition of $Li_2Si_2O_5$ whiskers, with the highest value (3.46 ± 0.10 $MPa{\cdot}m^{1/2}$) exhibited by the LDW5 samples. The increase in the fracture toughness of the LDWx ($x > 0$) samples may be related to the interlocking microstructure of coexisting elongated $Li_2Si_2O_5$ crystals with smaller ones, which was related to crack bridging and crack deflection. A microstructure consisting of bimodal crystal size distributions could cause crack blunting or branching, which was advantageous for enhancing the mechanical properties. The presence of rod-like whiskers was equivalent to a bridge between two crack surfaces and provided a force that brought the crack surfaces close to each other, which canceled out the effect of applied stress to a certain extent and significantly reduced the strength of the effective stress field at the crack tip. As the crack expanded further, the increase in the distance between the crack surfaces was bound to be

inhibited and constrained by the bridge action of the crystals, which increased the crack propagation resistance of the material. The crack-propagated in the glass matrix and through some small crystals, while it was deflected by large crystals. As seen in **Figure 3**, the LDW5 sample had a large amount of abnormally enlarged $Li_2Si_2O_5$ crystals (L_{max} of 6.81 μm, and W_{max} of 1.83 μm), which resulted in a larger angle of crack deflection. This deflection meant that the cracks had to surmount this additional surface area as they progressed through the material. As a result, more energy was absorbed, which contributed to the purpose of increasing the toughness. Consequently, LDWx ($x > 0$) in the present study had a better fracture toughness than LDW0.

Table 2 compares the mechanical properties of the $Li_2Si_2O_5$ whisker-reinforced glass-ceramics investigated in this work with those of other reported studies. The three-point flexural strength was higher than conventional sintered $Li_2Si_2O_5$ glass-ceramics and even comparable to commercial IPS e.max Press and IPS e.max CAD (Ivoclar Vivadent, Liechtenstein), with flexural strengths reaching 400 and 360 MPa according to the manufacturer's specifications, respectively. The fracture toughness of LDW5 was superior to those of most reported studies, including IPS e.max Press (2.75 $MPa{\cdot}m^{1/2}$) and IPS e.max CAD (2.25 $MPa{\cdot}m^{1/2}$). Thus, we improved the mechanical properties of $Li_2Si_2O_5$ glass-ceramics by adding $Li_2Si_2O_5$ whiskers. The results showed that $Li_2Si_2O_5$ whisker reinforcement has great potential in improving the mechanical properties of $Li_2Si_2O_5$ glass-ceramics.

4 CONCLUSION

In this study, we reported a simple hydrothermal approach for the synthesis of $Li_2Si_2O_5$ whiskers. High-performance $Li_2Si_2O_5$ glass-ceramics with bimodal microstructures in which some large rod-like $Li_2Si_2O_5$ crystals and fine crystals were embedded in the glass matrix were prepared by adding $Li_2Si_2O_5$ whiskers directly into glass powders. Some large rod-like $Li_2Si_2O_5$ crystals epitaxially grew along with the whiskers, and small crystals directly crystallized from the parent glass powders. With an increase in the amount of $Li_2Si_2O_5$ whiskers, the crystallinity increased slightly, and the average crystal size also increased. The microstructure, with a bimodal crystal size distribution, contributed to high mechanical properties. The $Li_2Si_2O_5$ glass-ceramics exhibited high flexural strength (389.5 ± 11.77 MPa, LDW3) and fracture toughness (3.46 ± 0.10 $MPa{\cdot}m^{1/2}$, LDW5). The former resulted from a high crystallinity, low porosity, and appropriate crystal size, while the latter was mainly attributed to crack deflection and bridging by large, elongated $Li_2Si_2O_5$ crystals. These findings indicate that the obtained $Li_2Si_2O_5$ glass-ceramics offer a new route for the preparation of toughened glass-ceramics, which lays the foundation for clinical applications, especially for three-unit posterior-bridge prosthetics.

DATA AVAILABILITY STATEMENT

The original contributions presented in the study are included in the article/Supplementary Material, further inquiries can be directed to the corresponding author.

AUTHOR CONTRIBUTIONS

JY and XL contributed to the conceptualization, methodology, experiment, data analysis, and manuscript preparation. XW contributed to the investigation. XW, YZ, and BL contributed to the formal analysis and manuscript review. All authors have read and approved the content of the manuscript.

FUNDING

This research was funded by the Open Project of Shanxi Provincial Key Laboratory of Oral Disease Prevention and Treatment and New Materials, grant number KF2020-03; and the Scientific Research Funding Project for Returned Scholars of Shanxi Province, grant number HGKY2019-055, College Science and Technology Innovation Project of Shanxi Education Department, grant number 2020L0210.

ACKNOWLEDGMENTS

The authors would like to thank BL and YZ for their valuable discussions and feedback. The authors would also like to express their gratitude for the support from the Shanxi Province Key Laboratory of Oral Diseases Prevention and New Materials.

REFERENCES

Albakry, M., Guazzato, M., and Swain, M. V. (2004). Influence of Hot Pressing on the Microstructure and Fracture Toughness of Two Pressable Dental Glass-Ceramics. *J. Biomed. Mater. Res.* 71B, 99–107. doi:10.1002/jbm.b.30066

Alemi, A., Khademinia, S., Joo, S. W., Dolatyari, M., Bakhtiari, A., Moradi, H., et al. (2014a). Hydrothermal Synthesis and Investigation of Optical Properties of Nb5+-Doped Lithium Silicate Nanostructures. *Int. Nano. Lett.* 4, 1–10. doi:10.1007/s40089-014-0100-0

Alemi, A., Khademinia, S., and Sertkol, M. (2014b). Lithium Disilicate ($Li_2Si_2O_5$): Mild Condition Hydrothermal Synthesis, Characterization and Optical Properties. *J. Nanostruct.* 4, 407–412. doi:10.7508/jns.2014.04.001

Belli, R., Wendler, M., Cicconi, M. R., de Ligny, D., Petschelt, A., Werbach, K., et al. (2018). Fracture Anisotropy in Texturized Lithium Disilicate Glass-Ceramics. *J. Non-Crystalline Sol.* 481, 457–469. doi:10.1016/j.jnoncrysol.2017.11.040

Chen, X.-P., Xiang, Z.-X., Song, X.-F., and Yin, L. (2020). Machinability: Zirconia-Reinforced Lithium Silicate Glass Ceramic versus Lithium Disilicate Glass Ceramic. *J. Mech. Behav. Biomed. Mater.* 101, 103435. doi:10.1016/j.jmbbm.2019.103435

Elsaka, S. E., and Elnaghy, A. M. (2016). Mechanical Properties of Zirconia Reinforced Lithium Silicate Glass-Ceramic. *Dental Mater.* 32, 908–914. doi:10.1016/j.dental.2016.03.013

Fernandes, H. R., Tulyaganov, D. U., Goel, A., and Ferreira, J. M. F. (2012). Effect of K2O on Structure-Property Relationships and Phase Transformations in Li2O-SiO2 Glasses. *J. Eur. Ceram. Soc.* 32, 291–298. doi:10.1016/j.jeurceramsoc.2011.09.017

Fu, L., Engqvist, H., and Xia, W. (2020). Glass-ceramics in Dentistry: A Review. *Materials* 13, 1049. doi:10.3390/ma13051049

Hallmann, L., Ulmer, P., Gerngross, M.-D., Jetter, J., Mintrone, M., Lehmann, F., et al. (2019). Properties of Hot-Pressed Lithium Silicate Glass-Ceramics. *Dental Mater.* 35, 713–729. doi:10.1016/j.dental.2019.02.027

Hallmann, L., Ulmer, P., and Kern, M. (2018). Effect of Microstructure on the Mechanical Properties of Lithium Disilicate Glass-Ceramics. *J. Mech. Behav. Biomed. Mater.* 82, 355–370. doi:10.1016/j.jmbbm.2018.02.032

Huang, S., Cao, P., Li, Y., Huang, Z., and Gao, W. (2013). Nucleation and Crystallization Kinetics of a Multicomponent Lithium Disilicate Glass by *In Situ* and Real-Time Synchrotron X-ray Diffraction. *Cryst. Growth Des.* 13, 4031–4038. doi:10.1021/cg400835n

Huang, X., Zheng, X., Zhao, G., Zhong, B., Zhang, X., and Wen, G. (2014). Microstructure and Mechanical Properties of Zirconia-Toughened Lithium Disilicate Glass-Ceramic Composites. *Mater. Chem. Phys.* 143, 845–852. doi:10.1016/j.matchemphys.2013.10.023

Hussain, I., Barimah, E. K., Iqbal, Y., Jose, G., Zeb, A., and Muhammad, R. (2021). Mechanical and Optical Properties of ZrO2 Doped Silicate Glass Ceramics. *Silicon* 13, 877–883. doi:10.1007/s12633-020-00516-z

Kirsten, J., Belli, R., Wendler, M., Petschelt, A., Hurle, K., and Lohbauer, U. (2020). Crack Growth Rates in Lithium Disilicates with Bulk (Mis)alignment of the Li2Si2O5 Phase in the [001] Direction. *J. Non-Crystalline Sol.* 532, 119877. doi:10.1016/j.jnoncrysol.2019.119877

Kwon, S. J., Lawson, N. C., McLaren, E. E., Nejat, A. H., and Burgess, J. O. (2018). Comparison of the Mechanical Properties of Translucent Zirconia and Lithium Disilicate. *The J. Prosthetic Dentistry* 120, 132–137. doi:10.1016/j.prosdent.2017.08.004

Leenakul, W., and Kraipok, A. (2021). Effect of Increasing the Al2O3 Content on the Phase Formation and Mechanical Properties of Lithium Disilicate Glass-Ceramics. *Mater. Res. Express* 8, 055202. doi:10.1088/2053-1591/abffa1

Li, D., Guo, J. W., Wang, X. S., Zhang, S. F., and He, L. (2016). Effects of crystal Size on the Mechanical Properties of a Lithium Disilicate Glass-Ceramic. *Mater. Sci. Eng. A* 669, 332–339. doi:10.1016/j.msea.2016.05.068

Liu, X., Yan, J., Wu, X., Zhang, Y., and Li, B. (2022). Biosafety Evaluation of $Li_2Si_2O_5$ Whisker-Reinforced Glass-Ceramics. *Biomed. Mater.* 17, 025011. doi:10.1088/1748-605X/ac4e65

Liang, X., Li, Y., Wang, Q., Sang, S., Xu, Y., Chen, Y., et al. (2017). A Nitride Whisker Template for Growth of Mullite in SiC Reticulated Porous Ceramics. *Ceramics Int.* 43, 11197–11203. doi:10.1016/j.ceramint.2017.05.169

Lien, W., Roberts, H. W., Platt, J. A., Vandewalle, K. S., Hill, T. J., and Chu, T.-M. G. (2015). Microstructural Evolution and Physical Behavior of a Lithium Disilicate Glass-Ceramic. *Dental Mater.* 31, 928–940. doi:10.1016/j.dental.2015.05.003

Lodesani, F., Menziani, M. C., Maeda, K., Takato, Y., Urata, S., and Pedone, A. (2020). Disclosing crystal Nucleation Mechanism in Lithium Disilicate Glass through Molecular Dynamics Simulations and Free-Energy Calculations. *Sci. Rep.* 10, 17867. doi:10.1038/s41598-020-74764-9

Montazerian, M., and Zanotto, E. D. (2017). Bioactive and Inert Dental Glass-Ceramics. *J. Biomed. Mater. Res.* 105, 619–639. doi:10.1002/jbm.a.35923

Pinto, H., Ito, L., Crovace, M., Ferreira, E. B., Fauth, F., Wroblewski, T., et al. (2007). Surface and Bulk Residual Stresses in Li2O·2SiO2 Glass-Ceramics. *J. Non-Crystalline Sol.* 353, 2307–2317. doi:10.1016/j.jnoncrysol.2007.04.007

Serbena, F. C., Mathias, I., Foerster, C. E., and Zanotto, E. D. (2015). Crystallization Toughening of a Model Glass-Ceramic. *Acta Materialia* 86, 216–228. doi:10.1016/j.actamat.2014.12.007

Serbena, F. C., and Zanotto, E. D. (2012). Internal Residual Stresses in Glass-Ceramics: A Review. *J. Non-Crystalline Sol.* 358, 975–984. doi:10.1016/j.jnoncrysol.2012.01.040

Sun, Y., Ma, L., Cui, J., Feng, L., Zhang, Z., Yang, Y., et al. (2021). Effects of Heat-Treatment Temperature and Holding Time on the Microstructure and Mechanical Properties of Lithium Disilicate Glass-Ceramics. *J. Non-Crystalline Sol.* 553, 120502. doi:10.1016/j.jnoncrysol.2020.120502

Thieme, K., and Rüssel, C. (2014). Nucleation Inhibitors-The Effect of Small Concentrations of Al2O3, La2O3 or TiO2 on Nucleation and Crystallization of Lithium Disilicate. *J. Eur. Ceram. Soc.* 34, 3969–3979. doi:10.1016/j.jeurceramsoc.2014.06.008

von Clausbruch, S. C., Schweiger, M., Höland, W., Rheinberger, V., and Rheinberger, V. M. (2000). The Effect of P2O5 on the Crystallization and Microstructure of Glass-Ceramics in the SiO2-Li2O-K2o-ZnO-P2o5 System. *J. Non-Crystalline Sol.* 263-264, 388–394. doi:10.1016/S0022-3093(99)00647-X

Wang, F., Chai, Z., Deng, Z., Gao, J., Wang, H., and Chen, J. (2015). Effect of Heat-Pressing Temperature and Holding Time on the Microstructure and Flexural Strength of Lithium Disilicate Glass-Ceramics. *PloS one* 10, e0126896. doi:10.1371/journal.pone.0126896

Wen, G., Zheng, X., and Song, L. (2007). Effects of P2O5 and Sintering Temperature on Microstructure and Mechanical Properties of Lithium Disilicate Glass-Ceramics. *Acta Materialia* 55, 3583–3591. doi:10.1016/j.actamat.2007.02.009

Yuan, K., Wang, F., Gao, J., Sun, X., Deng, Z., Wang, H., et al. (2013). Effect of Sintering Time on the Microstructure, Flexural Strength and Translucency of Lithium Disilicate Glass-Ceramics. *J. Non-Crystalline Sol.* 362, 7–13. doi:10.1016/j.jnoncrysol.2012.11.010

Zhang, F., Reveron, H., Spies, B. C., Van Meerbeek, B., and Chevalier, J. (2019). Trade-off between Fracture Resistance and Translucency of Zirconia and Lithium-Disilicate Glass Ceramics for Monolithic Restorations. *Acta Biomater.* 91, 24–34. doi:10.1016/j.actbio.2019.04.043

Zhang, Y., Guo, H., Zhang, H., Deng, Y., Wang, B., and Yang, J. (2018a). Effect of Added Mullite Whisker on Properties of Lithium Aluminosilicate (LAS) Glass-Ceramics Prepared for Dental Restoration. *J. Biomed. Nanotechnol.* 14, 1944–1952. doi:10.1166/jbn.2018.2637

Zhang, Z., Guo, J., Sun, Y., Tian, B., Zheng, X., Zhou, M., et al. (2018b). Effects of crystal Refining on Wear Behaviors and Mechanical Properties of Lithium Disilicate Glass-Ceramics. *J. Mech. Behav. Biomed. Mater.* 81, 52–60. doi:10.1016/j.jmbbm.2018.02.023

Zhao, T., Li, A.-J., Qin, Y., Zhu, J.-F., Kong, X.-G., and Yang, J.-F. (2019). Influence of SiO2 Contents on the Microstructure and Mechanical Properties of Lithium Disilicate Glass-Ceramics by Reaction Sintering. *J. Non-Crystalline Sol.* 512, 148–154. doi:10.1016/j.jnoncrysol.2019.02.015

Zhao, T., Lian, M.-M., Qin, Y., Zhu, J.-F., Kong, X.-G., and Yang, J.-F. (2021). Improved Performances of Lithium Disilicate Glass-Ceramics by Seed Induced Crystallization. *J. Adv. Ceram.* 10, 614–626. doi:10.1007/s40145-021-0463-4

Zheng, X., Wen, G., Song, L., and Huang, X. X. (2008). Effects of P2O5 and Heat Treatment on Crystallization and Microstructure in Lithium Disilicate Glass Ceramics. *Acta Materialia* 56, 549–558. doi:10.1016/j.actamat.2007.10.010.1016/j.actamat.2007.10.024

Conflict of Interest: The authors declare that the research was conducted in the absence of any commercial or financial relationships that could be construed as a potential conflict of interest.

Publisher's Note: All claims expressed in this article are solely those of the authors and do not necessarily represent those of their affiliated organizations, or those of the publisher, the editors and the reviewers. Any product that may be evaluated in this article, or claim that may be made by its manufacturer, is not guaranteed or endorsed by the publisher.